Depot-dependent peroxisome response in the rat white adipose tissue under hypothyroidism

Ahsein Addloli,[1] Marija Ilic,[1] Tamara Zakic,[2] Bato Korac,[2] Aleksandra Cvoro,[1] Aleksandra Jankovic,[2] Aleksandra Korac[1]

[1]Center for Electron Microscopy, Faculty of Biology, Institute of Zoology, University of Belgrade
[2]Department of Physiology, Institute for Biological Research "Sinisa Stankovic", National Institute of Republic of Serbia, University of Belgrade, Serbia

ABSTRACT

The effect of thyroid hormones (TH) on metabolism and energy balance relies on their impact on lipid storage in adipose tissue (AT). Since peroxisomes play a key role in lipid metabolism in white AT, hypothyroidism may critically influence peroxisome population/dynamics. This study aimed to determine depot- and time-dependent effects of methimazole-induced hypothyroidism on peroxisome biogenesis and remodeling in rat white AT. Hypothyroidism was induced using 0.04% methimazole over 7, 15, or 21 days. We show that hypothyroidism affects peroxisome biogenesis in subcutaneous AT (SAT) and visceral AT (VAT) (mesenteric-mVAT, retroperitoneal-rVAT and gonadal-gVAT) in a depot-specific manner. Firstly, although a gradual increase in peroxisomal number is present in all of the AT depots examined, the time course differs. Secondly, according to ultrastructural and protein expression analyses of Pex11β, Pex19, and PPARα, biogenesis pathways are switching from canonical to *de novo* pathway in hypothyroidism, again distinctively across particular depots. Furthermore, this is accompanied by the emergence of unusual peroxisomal structures (pexopodium) infiltrating lipid bodies in VAT. The absence of acyl-coenzyme A oxidase 1 (ACOX1) suggests that such structures may develop as a consequence of uncoordinated oxidation of accumulated fatty acids in VAT. The presence of pexopodium was increased from day 15 of hypothyroidism in mVAT. However, this increase was transient in rVAT and gVAT, indicating different peroxisomal dynamics between VAT depots during the monitored period of induction. Pexopodium-like structures were not observed in SAT. Our results identify peroxisomal remodeling as a previously underappreciated component of adipose tissue plasticity in hypothyroidism. Discrete temporal and depot-specific responses, including the formation of pexopodia in VAT, underscore the functional heterogeneity of white AT depots and suggest that peroxisomal dynamics may contribute to regional metabolic vulnerability under thyroid hormone deficiency over the time.

Key words: rat white adipose tissue; visceral; subcutaneous; hypothyroidism; peroxisome; transmission electron microscopy.

Correspondence: Aleksandra Korac, Center for Electron Microscopy, Chair of Cell and Tissue Biology, University of Belgrade-Faculty of Biology, Studentski trg 16, 11000 Belgrade, Serbia. E-mail: aleksandra.korac@bio.bg.ac.rs

Contributions: Ahsein Addloli, data curation, formal analysis, writing - original draft. Marija Ilic, formal analysis, writing - original draft. Tamara Zakic, formal analysis. Bato Korac, conceptualization, writing - original draft, writing - review & editing. Aleksandra Cvoro, formal analysis, writing - original draft, writing - review & editing. Aleksandra Jankovic, formal analysis, writing - original draft, writing - review & editing. Aleksandra Korac, conceptualization, formal analysis, writing - original draft, writing - review & editing. All authors read and approved the final version of the manuscript and agreed to be accountable for all aspects of the work.

Conflict of interest: the authors declare no competing interests.

Ethical approval: the experiment has been conducted under the authorization of the Ethic Committee for the treatment of experimental animals of the Faculty of Biology at the University of Belgrade and by the Veterinary Directorate of the Ministry of Agriculture and Environmental Protection of the Republic of Serbia, with the document no. 323-07-07505/20l5-05/4).

Availability of data and materials: the datasets used and/or analyzed during the current study are available upon reasonable request from the corresponding author.

Funding: this research was supported by the Ministry of Science, Technological Development, and Innovation of the Republic of Serbia (grant numbers 451-03-33/2026-03/200178, 451-03-34/2026-03/200178 and 451-0333/2026-03/200007).

Acknowledgements: the authors would thank Samantha E. Armstrong for her diligent proofreading and assistance with the English language editing of this article.

Introduction

Thyroid hormones play an essential role in metabolic homeostasis and energy expenditure. Their deficiency (hypothyroidism), causes a broad spectrum of physiological changes, most notably disruption of lipid metabolism.[1,2] Prolonged hypothyroidism induces white adipose tissue (AT) dysfunction, particularly impacting visceral AT (VAT),[3] which contributes to ectopic lipid deposition and dyslipidemia.[4] Thus, enhanced insight into the regulation of lipid storage and oxidation in white AT is critical for preventing metabolic complications associated with hypothyroidism.[5-7]

Peroxisomes are involved in the synthesis of triacylglycerols and ether lipids as well as fatty acid oxidation in white AT. Simultaneously, peroxisomes produce important lipid and redox signaling molecules, synchronizing lipid release through fatty acid metabolism and adipogenesis.[8-10] In addition, distinct white AT depots have unique profiles regarding adipogenesis, adipocyte size,[11,12] lipolysis,[13] glucose uptake, oxidation, and incorporation in triacylglycerols,[14] as well as oxidative and antioxidant capacity,[15] both under basal conditions and in response to dietary and hormonal changes. Hence, peroxisomes also exhibit dynamic, depot-specific regulation of redox homeostasis and adipocyte metabolism[10], and their changing numbers, occurrences, and localizations over time likely reflect the pathophysiological response of white AT in hypothyroidism.[5-7] In particular, hypothyroidism causes a 2.4-fold decrease in peroxisomal β-oxidation in the subcellular fraction of white AT (epididymal and perirenal depots).[16]

Peroxisomal biogenesis and maturation are mediated by a family of proteins known as peroxins. Although evolutionally conserved, these proteins exhibit species-specific characteristics. In rodents, Pex11β coordinates peroxisome proliferation,[17] while Pex19 is crucial for both the division of pre-existing peroxisomes and the *de novo* formation of peroxisomes from the endoplasmic reticulum.[18] In this manner, Pex11β and Pex19 characterize the two established pathways of peroxisomal biogenesis: the *de novo* pathway and the canonical pathway from pre-existing peroxisomes.

The peroxisome proliferator activated receptor alpha (PPARα) is a transcription factor that plays a key role in the regulation of lipid metabolism. It is the crucial control point impacting fatty acid uptake, fatty acid activation, intracellular fatty acid binding, mitochondrial and peroxisomal fatty acid oxidation, triacylglycerol turnover, and lipid droplet biology.[19] Furthermore, recent data emphasize the key role of peroxisomal β-oxidation in sensing PPARα-dependent lipid and energy metabolism.[20] In this context, PPARα acts as a lipid-sensing transcriptional hub that integrates fatty acid flux with peroxisomal abundance.[21] Upon activation, PPARα not only induces the enzymatic machinery of peroxisomal β-oxidation, including acyl-CoA oxidase 1 (ACOX1),[22,23] but also promotes peroxisome proliferation through transcriptional regulation of genes involved in membrane remodeling and organelle dynamics, particularly members of the PEX11 family.[24,25] Moreover, components of the peroxisomal biogenesis machinery are transcriptionally responsive to PPARα signaling, further linking lipid sensing to the canonical pathway of peroxisome biogenesis.[26] Through this coordinated regulation of metabolic enzymes and peroxisomal biogenic factors, PPARα aligns organelle oxidative capacity with cellular lipid availability and energetic demand. Notably, PPARα tissue expression is ubiquitous, although not uniform. PPARα is predominantly expressed in tissues with high rates of fatty acid catabolism, and is comparatively low in white AT depots.[27,28] This inherently low PPARα expression in white AT becomes particularly relevant under hypothyroid conditions.

Subcutaneous AT (SAT) and VAT display distinct divergence in organelle-level remodeling during various metabolic changes, which underlie their different roles in metabolism and disease risk.[29,30] Although peroxisomes are well-established as key organelles in lipid metabolism and redox regulation in adipocytes,[11] and they interact directly with mitochondria and lipid bodies to influence metabolic remodeling, understanding of how these interactions differ specifically between SAT and VAT remains limited.

Our study aimed to investigate the impact of hypothyroidism on the peroxisomal population in the SAT and different VAT depots (mesenteric-mVAT, retroperitoneal-rVAT and gonadal-gVAT). To this end, we investigated peroxisome biogenesis at the ultrastructural level and tracked the expression of key peroxisomal biogenesis proteins Pex11β and Pex19 and transcriptional factor PPARα, in rats during methimazole-induced hypothyroidism.

Materials and Methods

Animals and experimental design

Two-month-old male Wistar rats (330±30 g) were maintained under 22±1°C and 12 h light/dark cycles with *ad libitum* access to standard pelleted food. Animals were divided into four groups, each consisting of 8 animals. To induce hypothyroidism, three groups of animals were administered 0.04% methimazole (Methimazole crystalline M8506; Sigma Aldrich Chemie GmbH, Taufkirchen, Germany) *via* their drinking water for 7, 15, or 21 days. This treatment led to a decrease in serum triiodothyronine and thyroxine concentrations by 2-fold and 5 to 6-fold, respectively, and increase in thyroid-stimulating hormone level by 5 to 6-fold.[31] The fourth group of tap-water-drinking animals served as the euthyroid control. At the end of the experiment, animals were sacrificed using a decapitator (Harvard Apparatus, Holliston, MA, USA), and depots of white AT were isolated and processed for microscopy and Western blot. The experiment has been conducted under the authorization of the Ethic Committee for the treatment of experimental animals of the Faculty of Biology at the University of Belgrade and by the Veterinary Directorate of the Ministry of Agriculture and Environmental Protection of the Republic of Serbia, with the document no. 323-07-07505/2015-05/4).

Transmission electron microscopy

Small parts of SAT depo and VAT depots (rVAT, rVAt and gVAT) immediately after dissection were fixed with 2% glutaraldehyde/2% paraformaldehyde in 0.1 M Sørensen phosphate buffer (PB), pH 7.2 for 1h at 4°C. After fixation, tissue was rinsed in PB and then preincubated in 0,1% 3, 3'- diaminobenzidine (DAB) in PB for 30 minutes, for peroxidase staining.[32] Then, 0.01% H_2O_2 was added to the preincubation medium and incubated for 1h at 37°C. After washing in PB, tissue was postfixed in 2% osmium tetroxide in the same buffer, then routinely dehydrated and embedded in Araldite. Other portions of the same SAT and VAT depot samples were routinely fixed in 2.5% glutaraldehyde in 0.1 M Sørensen PB for 1h at 4°C, postfixed in 2% osmium tetroxide in the same buffer, and routinely dehydrated and embedded in Araldite. Ultra-thin sections of white AT depots were obtained using a Leica UC6 ultramicrotome (Leica Microsystems, Wetzlar, Germany) and mounted on copper grids. Sections were examined on a Philips CM12 transmission electron microscope (Philips/FEI, Eindhoven, The Netherlands) equipped with the digital camera SIS MegaView III (Olympus Soft Imaging Solutions, Münster, Germany).

Morphometric analyses

For each experimental group (N = 8), we used a digital camera SIS MegaView III (Olympus Soft Imaging Solutions) to capture electron microscopic images of 19 randomly selected white adipocytes at 17,000× magnification. We selected all white adipocytes to include both the nuclear and cytoplasmic areas. To overcome variations in white adipocyte size when quantifying peroxisomes, DAB-positive organelles were counted per cell area (μm^2), and subsequently normalized to a 100 μm^2 area.

Immunogold labeling

Ultra-thin sections of white AT depots routinely prepared for electron microscopy examination were obtained using a Leica UC6 ultramicrotome (Leica Microsystems) and mounted on nickel grids. After antigen retrieval in 10mM citrate buffer and incubation with 5% BSA in Tris-buffered saline/0.1% Tween 20 (TBS-T) for 1h at room temperature, grids were incubated overnight at 4°C with primary anti-ACOX1 antibody (1:50, ab184032). After rinsing in TBS-T, grids were incubated with 20-nm gold-conjugated anti-rabbit secondary antibody (1:20, ab27237), for 1h at room temperature, rinsed in TBS-T and double-distilled water, air-dried, and examined with a Philips CM12 transmission electron microscope (Philips/FEI, Eindhoven, The Netherlands). The specificity of the immune reactions was tested by omitting the primary antibody.

Western blotting

After decapitation, the right portion (rVAT, gVAT) or half portion (SAT, mVAT) of tissues was frozen immediately. Tissues were prepared according to Jankovic *et al*[33], and protein content was estimated.[34] The number of analyzed animals per group is N=3. Primary antibodies against: peroxisomal biogenesis factors 11β (Pex11β; 1:1000, ab74507), and 19 (Pex19; 1:2000, ab137072), PPARα (1:2000, ab8934) and β-actin (1:2000, ab8226) were purchased from Abcam (Cambridge, UK). Immunoreactive bands were quantified using ImageJ software (NIH, Bethesda, USA) and normalized against β-actin. The volume represents the sum of all pixel intensities within a band, and 1 pixel = 0.007744 mm^2. We averaged the ratio of pixels per band for the target protein in corresponding samples from three similar independent experiments.

Statistical analysis

All obtained data were analyzed by the software GraphPad Prism (GraphPad Prism, Version 8.4.3, San Diego, CA, USA). Normal distribution was tested by D'Agostino and Pearson's normality test. Analysis of variance with multiple comparisons (One-way ANOVA) with Dunnett's post hoc tests was used for evaluating the differences between groups. Results are expressed as mean ± SD of obtained values, and significances were set at $p<0.05$.

Results

Hypothyroidism instigates changes in peroxisome biogenesis in both SAT and VAT in a depot-specific manner

DAB-labeled peroxisomes were used to investigate peroxisomal abundance in white AT depots over the course of hypothyroidism. Thorough examination of electron micrographs and peroxisome quantification demonstrated an increase in peroxisomal number over the time in all analyzed white AT depots, yet with evident differences (Figure 1, Table 1). rVAT and gVAT of euthyroid controls exhibited a higher number of peroxisomes compared to mVAT and SAT controls. Hypothyroidism rapidly induced an increase in peroxisome number in all SAT and VAT depots (day 7). In gVAT, the number continued to rise steadily throughout the 24-day treatment, whereas in mVAT, rVAT and SAT, the changes were irregular. In all of the examined depots (SAT and VAT), peroxisome biogenesis predominantly proceeded via the canonical pathway, characterized by growth and division of existing elongated peroxisomes, as presented in Figure 2. However, hypothyroidism also activated the *de novo* pathway, characterized by peroxisomal budding from endoplasmic reticulum, in rVAT and gVAT, although in a different manner. In gVAT, the *de novo* pathway was observed only on day 7, while rVAT showed a more complex pattern. In rVAT, the *de novo* pathway was already functional in euthyroid control and was further enhanced by hypothyroidism, causing a time-dependent increase in peroxisomal number with the peak at day 15 (Figure 2). As peroxisomal biogenesis and/or functions require specific structural cooperation with endoplasmic reticulum, mitochondria or lipid body, we analyzed peroxisomal localisation within the cells. As expected, peroxisomes were located close to lipid body independently of either treatment or examined depots (SAT and VAT) (Figure 3). Additionally, they were often attached to mitochondria (Figure 3). Regarding the endoplasmic reticulum, its prominent presence was expectedly observed only in rVAT and in gVAT on day 7 as a consequence of *de novo* peroxisomal biogenesis (Figure 3, rVAT, gVAT).

Hypothyroidism modifies the expression of peroxins Pex11β and Pex19 in white AT depots

To understand peroxisomal biogenesis in AT in hypothyroidism, we assessed the protein levels of key peroxins, involved in peroxisomal proliferation (Pex11β) and membrane assembly (Pex19) (Figure 4). In general, hypothyroidism increased protein expression of both Pex11β and Pex19 in all examined AT depots, with differences observed over the time. In SAT, mVAT and gVAT, an increase in Pex11β level was evident after 7 days of treatment, while in rVAT, it was delayed (Figure 4). On the contrary, an increase in Pex19 expression took longer in all depots except mVAT (day 7).

Table 1. The average peroxisome number per 100 μm^2 area of white adipocytes.

Depot	Control	M7	M15	M21
SAT	3.188±0.274	5.395±0.674***	4.853±0.468***	6.836±0.721***
mVAT	2.404±0.612	6.891±0.780***	6.535±0.804***	8.242±1.020***
rVAT	3.891±0.590	5.943±0.831***	5.717±0.784***	6.233±0.771***
gVAT	4.812±0.592	6.464±0.932***	9.821±1.437***	10.894±1.652***

Mean values ± SD are represented. *Compared to the control value; ***$p<0.001$.

OPEN ACCESS

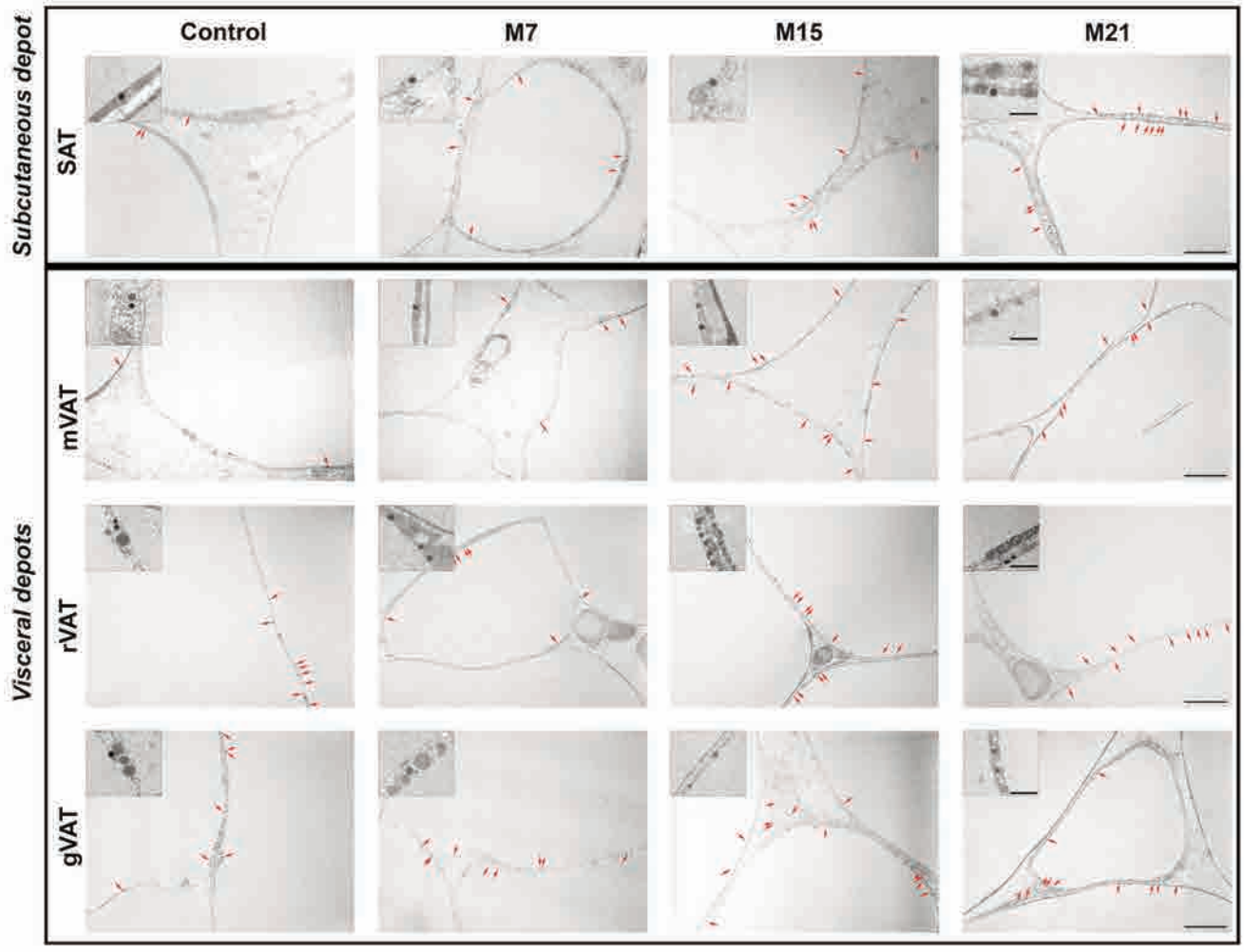

Figure 1. Representative electron micrographs of cytochemical labeled peroxisomes in SAT and VAT depots of white AT. Peroxisomes (arrow) were stained by DAB in white AT from control and hypothyroid rats treated with methimazole for 7, 15, or 21 days. Insets: magnified area with DAB-positive peroxisome. Scale bar: 2 μm; insets, 250 nm.

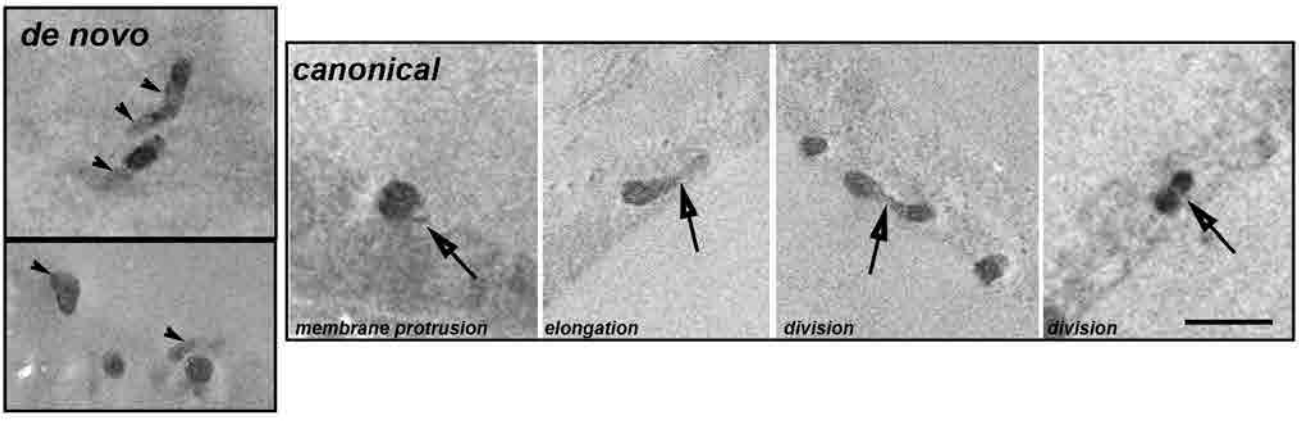

Figure 2. Peroxisome biogenesis in white adipocytes by *de novo* pathway and by the canonical pathway through growth and division. Representative electron micrograph with DAB-labeled peroxisomes in white adipocytes cytoplasm of VAT depots. *De novo* pathway (in gVAT on day 7 and in rVAT on day 15) is characterized by several interconnected peroxisomes (arrowhead) originating from endoplasmic reticulum. Canonical pathways present in all examined depots begins with the formation of a membrane protrusion followed by peroxisomal elongation and division (arrow). Scale bar: 250 nm.

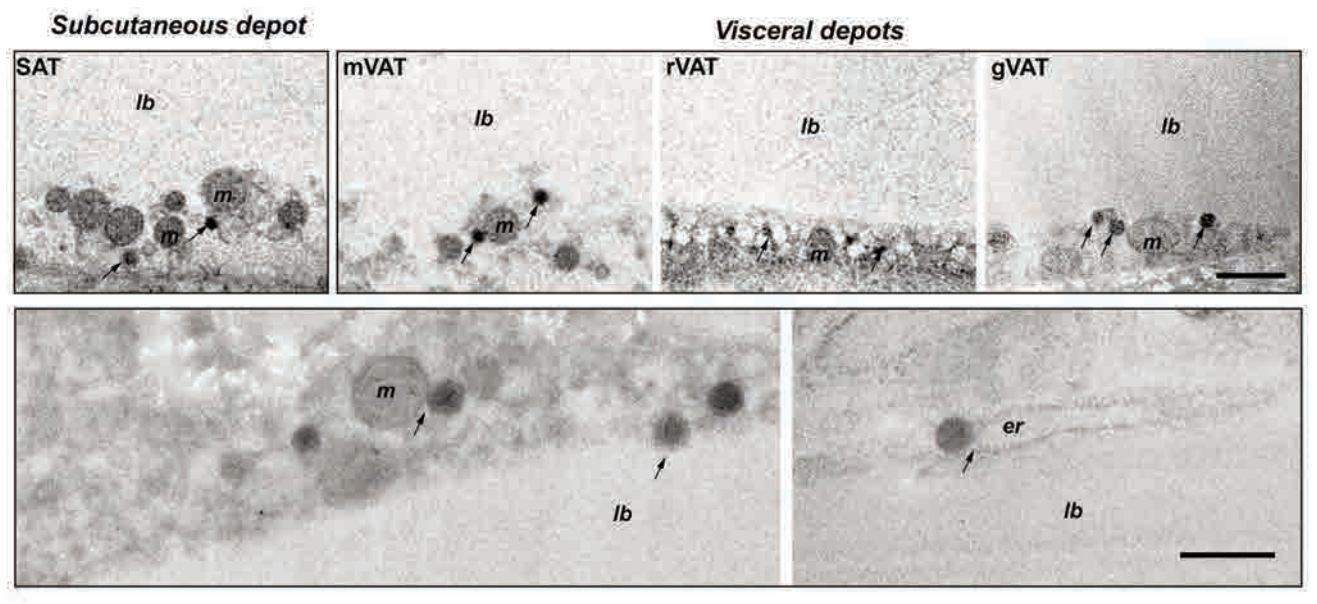

Figure 3. Localization of peroxisomes in white adipocytes after 7 days of methimazole treatment (first row). Peroxisomes (first row, arrow) are predominantly located adjacent to the lipid body (lb) or in their vicinity. Additionally, they are often attached to mitochondria (m). Magnified representative area (second row) shows contact (arrow) between peroxisome with mitochondria (m), lipid body (lb), or endoplasmic reticulum (er), respectively. Scale bar: first row, 1µm; second row, 500 nm.

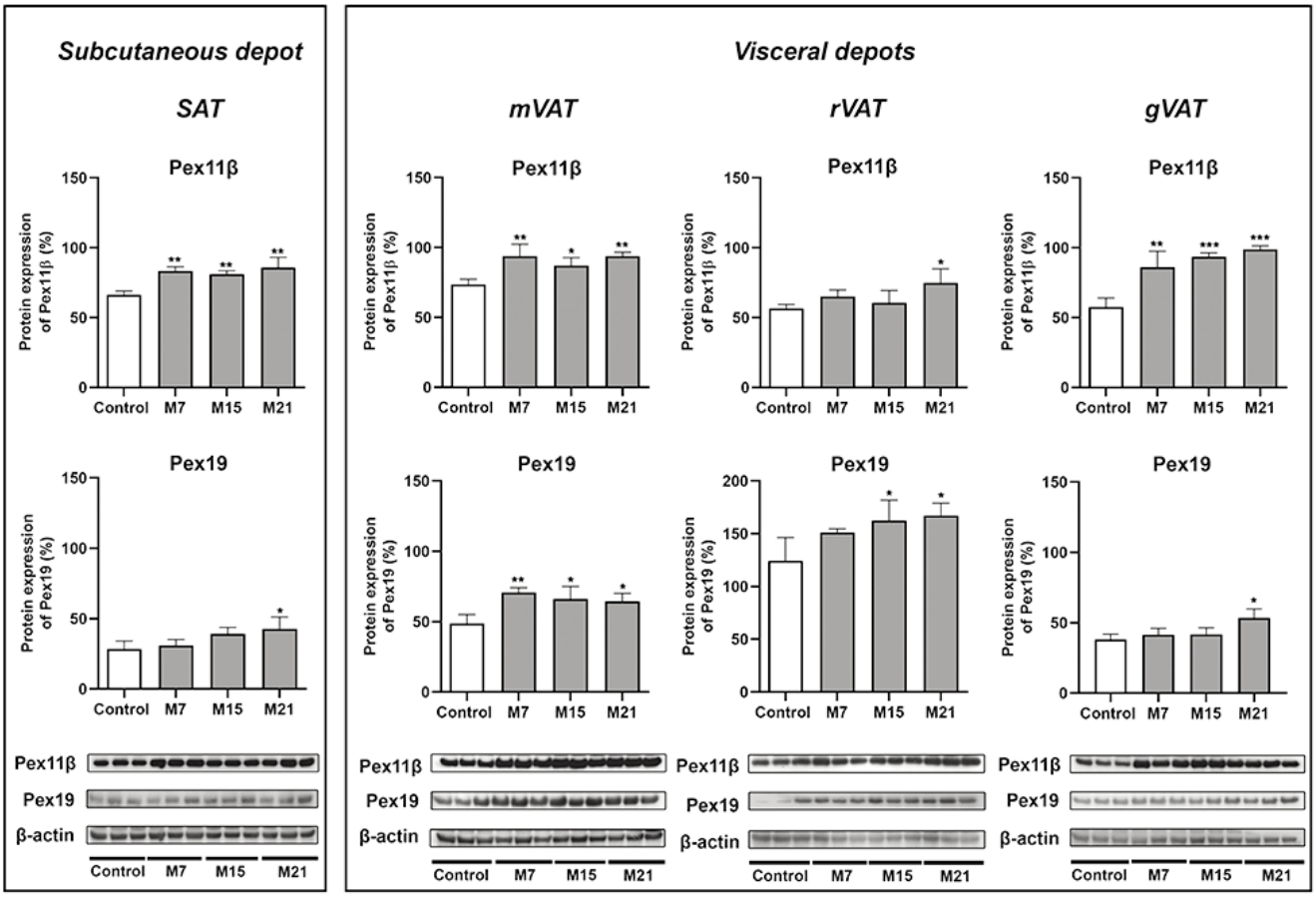

Figure 4. Protein expression of Pex11β and Pex19 in SAT and VAT depots of white AT from control (white) and hypothyroid (grey) groups treated with methimazole for 7, 15, or 21 days. Data shown represent the average values of target protein bands normalized against those of beta-actin, along with their representative blots (n=3 per group). *p<0.05, **p<0.01, ***p<0.001.

OPEN ACCESS

Hypothyroidism modifies PPARα protein expression differently in SAT and depots of VAT

PPARα basal expression was significantly higher in SAT and mVAT than in other VAT depots, and hypothyroidism did not cause any change in its expression (Figure 5). However, there was a significant increase in PPARα level in rVAT and gVAT during hypothyroidism. In gVAT, this increase was transient, occurring only on day 7 of treatment.

Hypothyroidism causes the emergence of a pexopodium-like structure in VAT but not in SAT

Numerous structures resembling peroxisomal protrusions – pexopodium were observed in all VAT depots, but not in a SAT (Figure 6). These pexopodium-like structures were visible toward the lipid body's interior in adipocytes with noticeable differences between different depots of VAT. The pexopodium-like structures (arrowhead) appeared only in visceral depots, in mVAT and rVAT from day 15 of hypothyroidism, and on day 21 in gVAT. They were DAB positive, larger than peroxisomes, and had a semi-spherical form (Figure 6). It has been assumed that they represent extension(s) of preexisting peroxisomes that enter the lipid bodies.[35] Additionally, they increase the contact surface of peroxisomes with lipid bodies due to the increased rate of lipolysis and provide more free fatty acids for oxidation.

Knowing the aforementioned role of pexopodium and giving their localization in lipid body and association with peroxisomes observed herein, we applied immunogold labeling of ACOX1, the first and rate-limiting enzyme in the peroxisomal β-oxidation pathway.[36] The labeling was performed at the time point and VAT depot with the highest appearance of the pexopodium-like structure (rVAT, M15). ACOX1 was found only in peroxisomes (arrows), while pexopodium-like structures did not show any immunopositivity (arrowhead) (Figure 7 A-D). However, some ACOX1 immunopositive peroxisomes were associated with pexopodium-like structures (Figure 7D, circle).

Discussion

This research provides new insights into depot-specific and time-dependent peroxisomal dynamics in white AT depots during methimazole-induced hypothyroidism in rats. Our findings demonstrate that methimazole treatment drives coordinated, but heterogeneous responses across white AT depots involving Pex11β/Pex19 and PPARα, which mediate an increase in peroxisome abundance over the course of treatment. Additionally, electron microscopy revealed distinct, depot-specific peroxisomal origins and the emergence of specific peroxisomal structures known as pexopodia. Although the role of these unique pexopodium-like structures in lipid oxidation has been proposed, our analysis of ACOX1 immunolocalization does not support their direct involvement in β-oxidation. Instead, the findings suggest that these structures reflect altered/aberrant fatty acid metabolism characteristic of hypothyroid conditions. These findings are discussed in detail below. Peroxisome-specific DAB labeling revealed a significant increase in peroxisome numbers in adipocytes of all analyzed AT depots. Further ultrastructural analysis demonstrated that peroxisomal biogenesis in both SAT and VAT depots occurs via two common pathways: the canonical, by growth and division, and the *de novo,* by budding from the smooth endoplasmic reticulum. The primary pathway in white AT depots is the canonical pathway. However, a clear depot- and time-dependent divergence was observed in the activation of these pathways.

Pex11β, the constitutively expressed isoform of the Pex11 family, regulates peroxisome proliferation and controls their morphology, size, and number.[37-42] It is the major peroxin that drives the canonical pathway of peroxisome biogenesis,[43] while Pex19 is a multifunctional protein essential for assembly of the peroxisomal membrane and import of peroxisomal membrane proteins.[44] In addition to its role in the canonical pathway, Pex19 has also been shown to play a role in *de novo* biogenesis. It is required for the budding of pre-peroxisomal vesicles from the endoplasmic reticu-

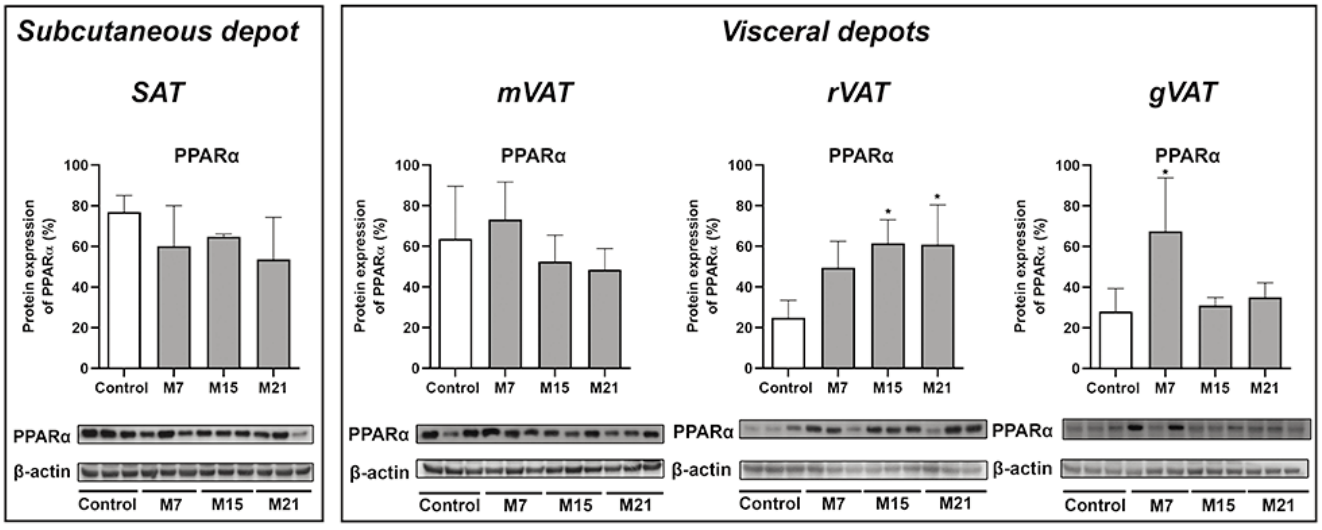

Figure 5. Protein expression of PPARα in SAT and VAT depots of AT from control (white) and hypothyroid (grey) groups treated with methimazole for 7, 15, or 21 days. Data shown represent the average values of target protein bands normalized against those of beta-actin, along with their representative blots (n=3 per group). *p<0.05.

lum.[45] Our investigation revealed a time-course increase in the expression of Pex11β and Pex19 in all white AT depots, pointing to the gradual peroxisomal biogenesis in white AT of hypothyroid rats. SAT and mVAT showed an early increase in Pex11β expression and predominantly relied on peroxisome division, whereas visceral depots, particularly rVAT and gVAT, exhibited delayed induction of Pex11β (in rVAT) and Pex19 (in gVAT), suggesting depot-specific temporal differences in the mechanisms regulating peroxisomal expansion.

In addition, *de novo* peroxisome biogenesis from the endoplasmic reticulum was ultrastructurally detected in both rVAT and gVAT, but at distinct, non-coincident time points of hypothyroidism, while in SAT and mVAT depots, *de novo* peroxisome biogenesis was not observed at all. These findings provide strong evidence for depot-specific alterations in peroxisome biogenesis triggered by hypothyroidism in white AT. The differences among distinct VAT depots are more pronounced than those observed between SAT and VAT. The significance of depot-specific variations in white AT during hypothyroidism remains undetermined. Peroxisome *de novo* biogenesis often involves increased Pex19 expression, but this pattern is not universal across all white AT depots, as shown by comparing inguinal and gVAT depots. Namely, cold exposure increases Pex19 expression in the inguinal depot but not in the gVAT depot.[46]

Peroxisomes closely interact with lipid bodies - dynamic, single phospholipid-monolayer organelles - to regulate cellular lipid homeostasis.[47-49] Specifically, the peroxisome bilayer and the lipid body monolayer may undergo hemifusion at points of physical contact to promote fatty acid transfer between these compartments. Consistent with their functional coupling, we observed close peroxisome-lipid body contacts across all examined time points. Within this context, a major finding of this study is the identification of pexopodium-like structures - peroxisomal extensions bridging to lipid bodies - which are uniquely present in visceral white adipocytes. While pexopodium structures were observed in VAT at various time points in the hypothyroid state, these structures were not present in SAT. This indicates a depot-specific structural adaptation of peroxisome-lipid droplet interactions, restricted to VAT under hypothyroid conditions.

Close physical contact between peroxisomes and lipid bodies is well documented in mammalian, yeast, and plant cells.[50-55] Detailed immunocytochemical and ultrastructural analyses have shown that, depending on the species and conditions, peroxisomes form DAB-positive, hemispherical membrane projections termed pexopodia,[52,56] peroxules[57,58] or gnarls[52] that enter the lipid body core. However, despite these observations in other experimental systems, the emergence and functional role of such structures in adipose tissue remain poorly understood. The presumed role of

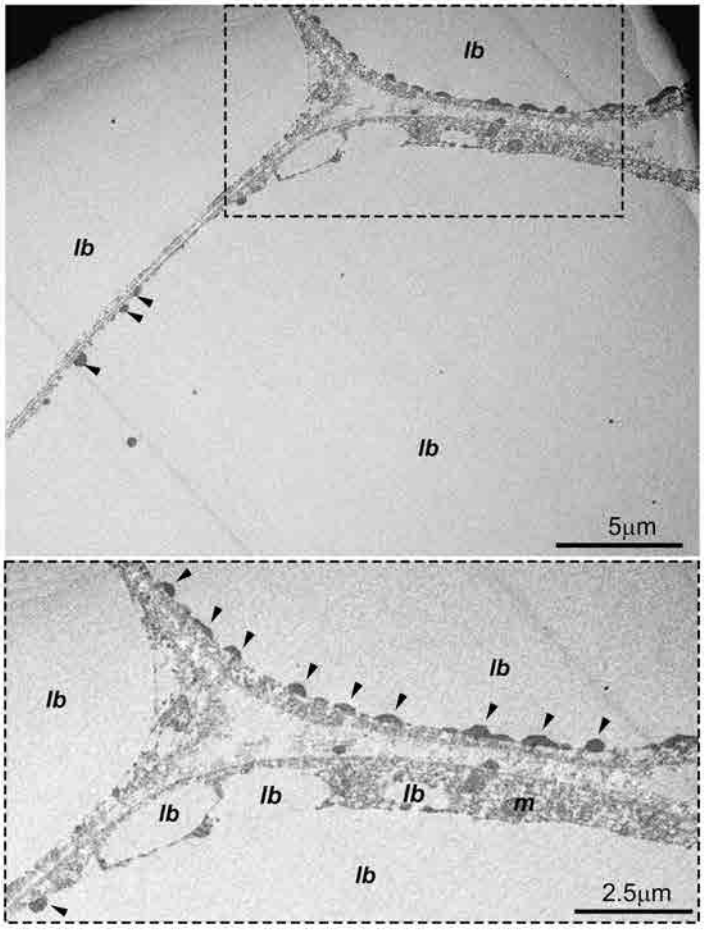

Figure 6. Presence of unusual pexopodium-like structures (arrow) that invaded lipid body's (lb) interior from their very surface was observed in white adipocytes. Pexopodium-like structures appeared in all VAT depots but not in the SAT depot. Representative electron micrographs from rVAT. Box represents magnified area. m-mitochondria. Scale bars: 2.5 µm and 5 µm.

OPEN ACCESS

these structures may be to increase the surface contact between peroxisomes and lipid bodies as shown in some studies,[35] resulting in accelerated lipolysis and increased free fatty acid availability for oxidation.[52]

Accordingly, an increase in PPARα protein levels was observed after 15 and 21 days of hypothyroidism in rVAT, i.e., after 7 days in gVAT, supporting the presumed role of pexopodia formation in fatty acid transfer and/or oxidation.[59] As the increase in PPARα was detected exclusively in adipose depots and coincided temporally with the presence of pexopodia, both features may reflect a common response of these AT depots characterized by enhanced fatty acid turnover, transport, and/or oxidation. However, further characterization of pexopodia through ACOX1 expression indicates that pexopodia, together with the observed elevated PPARα expression, may instead reflect an aberrant fatty acid oxidative VAT phenotype in hypothyroidism. Thus, to further characterize pexopodium-like structures, we examined ACOX1, the initial and rate-limiting enzyme of peroxisomal β-oxidation,[36] at its maximum level of manifestation in rVAT. Although ACOX1 was present in white adipocytes' peroxisomes, the pexopodium-like structures showed no immunogold-positivity. These results suggest that pexopodium-like structures are likely not involved in the β-oxidation of fatty acids, but potentially act as a depot for fatty acids and/or other lipid metabolites. Detailed profiling of enzymatic pathways involved in peroxisomal fatty acid α-oxidation and lipid synthesis should reveal the mechanisms and pathophysiological relevance of unusual peroxisomal structures in hypothyroid Our study demonstrates that SAT and VAT depots respond to hypothyroidism in distinct manner. SAT exhibited an early, division-driven increase in peroxisomes, while VAT depots responded later, using division followed by *de novo* biogenesis. This was accompanied by the appearance of pexopodium-like structures infiltrating lipid bodies at different time points, highlighting distinct functional peroxisomal differences within VAT depots during hypothyroidism.

The observed depot- and time-dependent variations in peroxisome appearance and formation, may provide a potential explanation for the location-specific responses of adipocytes to hypothyroidism. Importantly, this study expands current knowledge by revealing that white AT exhibits varied peroxisomal remodeling adaptations to hypothyroidism, rather than a uniform response. By identifying depot-specific structural and molecular adaptations of peroxisomes (peroxisome *vs* pexopodium-like structures, different biogenesis pathways, *etc*.), this study suggests a novel conceptual model for interpreting how thyroid-related metabolic imbalances[1-7] are driven by fat tissue heterogeneity.

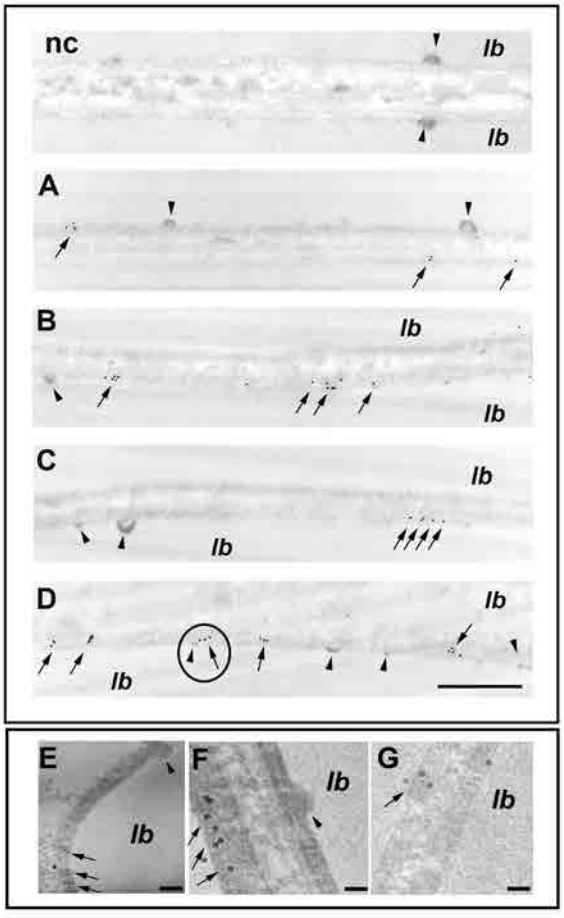

Figure 7. Immunogold labeling of ACOX1 in the rVAT adipocytes (**A-G**) after 15 days of methimazole treatment. While peroxisomes (arrow) are loaded with ACOX1, pexopodium-like structures (arrowhead) remain unlabeled. In some cases, an ACOX1-labeled peroxisome is associated with pexopodium-like structures (**D**, circle, arrowhead). nc, negative control; lb, lipid body. Scale bars: **A-D**) 1 μm; **E,G**) 100 nm.

References

1. Patel M, Mishra V, Pawar V, Ranvir R, Sundar R, Dabhi R. Evaluation of acute physiological and molecular alterations in surgically developed hypothyroid Wistar rats. J Pharmacol Pharmacother 2013;4:110-5.
2. Čakić-Milošević M, Korać A, Davidović Vukosava S. Methimazole-induced hypothyroidism in rats: Effects on body weight and histological characteristics of thyroid gland. Yug Med Biochem 2004;23:143-7.
3. López-Fontana CM, Pennacchio G, Zyla LE, Toneatto J, Bruna FA, Ortiz N, et al. Effects of hypothyroidism on the mesenteric and omental adipose tissue in rats. Mol Cell Endocrinol 2019;490:88-99.
4. Liu H, Peng D. Update on dyslipidemia in hypothyroidism: the mechanism of dyslipidemia in hypothyroidism. Endocr Connect 2022;11:e210002.
5. Blüher M. Adipose tissue dysfunction in obesity. Exp Clin Endocrinol Diabetes 2009;117:241-50.
6. Kusminski CM, Bickel PE, Scherer PE. Targeting adipose tissue in the treatment of obesity-associated diabetes. Nat Rev Drug Discov 2016;15:639-60.
7. Cho YK, Lee S, Lee J, Doh J, Park JH, Jung YS, Lee YH. Lipid remodeling of adipose tissue in metabolic health and disease. Exp Mol Med 2023;55:1955-73.
8. Lodhi IJ, Semenkovich CF. Peroxisomes: a nexus for lipid metabolism and cellular signaling. Cell Metab 2014;19:380-92.
9. Liu X, He A, Lu D, Hu D, Tan M, Abere A, et al. Peroxisomal metabolism of branched fatty acids regulates energy homeostasis. Nature 2025;646:1223-31.
10. Liu J, Lu W, Shi B, Klein S, Su X. Peroxisomal regulation of redox homeostasis and adipocyte metabolism. Redox Biol 2019;24:101167.
11. Wronska A, Kmiec Z. Structural and biochemical characteristics of various white adipose tissue depots. Acta Physiol (Oxf) 2012;205:194-208.
12. Sackmann-Sala L, Berryman DE, Munn RD, Lubbers ER, Kopchick JJ. Heterogeneity among white adipose tissue depots in male C57BL/6J mice. Obesity (Silver Spring) 2012;20:101-11.
13. Tchernof A, Bélanger C, Morisset AS, Richard C, Mailloux J, Laberge P, Dupont P. Regional differences in adipose tissue metabolism in women: minor effect of obesity and body fat distribution. Diabetes 2006;55:1353-60.
14. Festuccia WT, Blanchard PG, Turcotte V, Laplante M, Sariahmetoglu M, Brindley DN, Deshaies Y. Depot-specific effects of the PPARgamma agonist rosiglitazone on adipose tissue glucose uptake and metabolism. J Lipid Res 2009;50:1185-94.
15. Jankovic A, Korac A, Buzadzic B, Otasevic V, Stancic A, Daiber A, Korac B. Redox implications in adipose tissue (dys)function--A new look at old acquaintances. Redox Biol 2015;6:19-32.
16. Bas S, Giacobino JP. Peroxisomal and mitochondrial palmitoyl coenzyme A beta-oxidation activities in rat white adipose tissue and their regulation in hypothyroidism. Arch Biochem Biophys 1983;222:416-23.
17. Koch J, Pranjic K, Huber A, Brocard C. PEX11 family members are membrane elongation factors that coordinate peroxisome proliferation and maintenance. J Cell Sci 2010;123:3389-3400.
18. Agrawal G, Shang HH, Xia ZJ, Subramani S. Functional regions of the peroxin Pex19 necessary for peroxisome biogenesis. J Biol Chem 2017;292:11547-60.
19. Green S. PPAR: a mediator of peroxisome proliferator action. Mutat Res 1995;333:101-9.
20. Rakhshandehroo M, Knoch B, Müller M, Kersten S. Peroxisome proliferator-activated receptor alpha target genes. Biochim Biophys Acta 2010;1801:141-50.
21. Kersten S, Desvergne B, Wahli W. Roles of PPARs in health and disease. Nature 2000;405:421-4.
22. Issemann I, Green S. Activation of a member of the steroid hormone receptor superfamily by peroxisome proliferators. Nature 1990;347:645-50.
23. Tugwood JD, Issemann I, Anderson RG, Bundell KR, McPheat WL, Green S. The mouse peroxisomal acyl-CoA oxidase gene is activated by PPAR. EMBO J 1992;11:433-9.
24. Schrader M, Costello J, Godinho LF, Islinger M. Proliferation and fission of peroxisomes. Biochim Biophys Acta 2016;1863:971-83.
25. Li X, Baumgart E, Dong GX, Morrell JC, Jimenez-Sanchez G, Valle D, et al. PEX11α is required for peroxisome proliferation in response to PPARα activation. J Biol Chem 2002;277:5611-8.
26. Smith JJ, Aitchison JD. Peroxisomes take shape. Nat Rev Mol Cell Biol. 2013;14:803-17.
27. Tahri-Joutey M, Andreoletti P, Surapureddi S, Nasser B, Cherkaoui-Malki M, Latruffe N. Mechanisms mediating the regulation of peroxisomal fatty acid beta-oxidation by PPARα. Int J Mol Sci 2021;22:8969.
28. Dreyer C, Keller H, Mahfoudi A, Laudet V, Krey G, Wahli W. Positive regulation of the peroxisomal beta-oxidation pathway by fatty acids through activation of peroxisome proliferator-activated receptors (PPAR). Biol Cell 1993;77:67-76.
29. Soskic MB, Zakic T, Korac A, Korac B, Jankovic A. Metabolic remodeling of visceral and subcutaneous white adipose tissue during reacclimation of rats after cold. Appl Physiol Nutr Metab 2024;49:649-58.
30. Narita T, Kobayashi M, Itakura K, Itagawa R, Kabaya R, Sudo Y, et al. Differential response to caloric restriction of retroperitoneal, epididymal, and subcutaneous adipose tissue depots in rats. Exp Gerontol 2018;104:127-37.
31. Aleksic M, Golic I, Kalezic A, Jankovic A, Korac B, Korac A. Hypothyroidism intensifies both canonic and the de novo pathway of peroxisomal biogenesis in rat brown adipocytes in a time-dependent manner. Cells 2021;10:2248.
32. LeHir M, Herzog V, Fahimi HD. Cytochemical detection of catalase with 3,3'-diaminobenzidine. A quantitative reinvestigation of the optimal conditions. Histochemistry 1979;64:51-66.
33. Jankovic A, Korac A, Srdic-Galic B, Buzadzic B, Otasevic V, Stancic A et al. Differences in the redox status of human visceral and subcutaneous adipose tissues-relationships to obesity and metabolic risk. Metabolism 2014;63:661-71.
34. Lowry OH, Rosebrough NJ, Farr AL, Randall RJ. Protein measurement with the Folin phenol reagent. J Biol Chem 1951;193:265-75.
35. Carmichael RE, Richards DM, Fahimi HD, Schrader M. Organelle membrane extensions in mammalian cells. Biology (Basel) 2023;12:664.
36. Osumi T, Hashimoto T, Ui N. Purification and properties of acyl-CoA oxidase from rat liver. J Biochem 1980;87:1735-46.
37. Delille HK, Alves R, Schrader M. Biogenesis of peroxisomes and mitochondria: linked by division. Histochem Cell Biol 2009;131:441-6.
38. Koch A, Yoon Y, Bonekamp NA, McNiven MA, Schrader M. A role for Fis1 in both mitochondrial and peroxisomal fission

OPEN ACCESS

in mammalian cells. Mol Biol Cell 2005;16:5077-86.
39. Koch J, Pranjic K, Huber A, Ellinger A, Hartig A, Kragler F, Brocard C. PEX11 family members are membrane elongation factors that coordinate peroxisome proliferation and maintenance. J Cell Sci 2010;123:3389-400.
40. Li X, Gould SJ. PEX11 promotes peroxisome division independently of peroxisome metabolism. J Cell Biol 2002;156: 643-51.
41. Farré JC, Mahalingam SS, Proietto M, Subramani S. Peroxisome biogenesis, membrane contact sites, and quality control. EMBO Rep 2019;20:e46864.
42. Thoms S, Erdmann R. Dynamin-related proteins and Pex11 proteins in peroxisome division and proliferation. FEBS J 2005;272:5169-81.
43. Schrader M, Reuber BE, Morrell JC, Jimenez-Sanchez G, Obie C, Stroh TA, et al. Expression of PEX11beta mediates peroxisome proliferation in the absence of extracellular stimuli. J Biol Chem 1998;273:29607-14.
44. Jones JM, Morrell JC, Gould SJ. PEX19 is a predominantly cytosolic chaperone and import receptor for class 1 peroxisomal membrane proteins. J Cell Biol 2004;164:57-67.
45. Agrawal G, Subramani S. De novo peroxisome biogenesis: Evolving concepts and conundrums. Biochim Biophys Acta 2016;1863:892-901.
46. Park H, He A, Tan M, Johnson JM, Dean JM, Pietka TA, et al. Peroxisome-derived lipids regulate adipose thermogenesis by mediating cold-induced mitochondrial fission. J Clin Invest 2019;129:694-711.
47. Walther TC, Farese RV Jr. Lipid droplets and cellular lipid metabolism. Annu Rev Biochem 2012;81:687-714.
48. Welte MA. Expanding roles for lipid droplets. Curr Biol 2015;25:R470-81.
49. Olzmann JA, Carvalho P. Dynamics and functions of lipid droplets. Nat Rev Mol Cell Biol 2019;20:137-55.
50. Blanchette EJ. Ovarian steroid cells. II. The lutein cell. J Cell Biol 1966;31:517-42.
51. Aleksic M, Kalezic A, Saso L, Jankovic A, Korac B, Korac A. The unity of redox and structural remodeling of brown adipose tissue in hypothyroidism. Antioxidants (Basel) 2021;10:591.
52. Binns D, Januszewski T, Chen Y, Hill J, Markin VS, Zhao Y, et al. An intimate collaboration between peroxisomes and lipid bodies. J Cell Biol 2006;173:719-31.
53. Gao Q, Goodman JM. The lipid droplet-a well-connected organelle. Front Cell Dev Biol 2015;3:49.
54. Kunze M, Pracharoenwattana I, Smith SM, Hartig A. A central role for the peroxisomal membrane in glyoxylate cycle function. Biochim Biophys Acta 2006;1763:1441-52.
55. Schrader M. Tubulo-reticular clusters of peroxisomes in living COS-7 cells: dynamic behavior and association with lipid droplets. J Histochem Cytochem 2001;49:1421-9.
56. Goldberg AA, Bourque SD, Kyryakov P, Boukh-Viner T, Gregg C, Beach A, et al. A novel function of lipid droplets in regulating longevity. Biochem Soc Trans 2009;37:1050-5.
57. Scholz P, Chapman KD, Mullen RT, Ischebeck T. Finding new friends and revisiting old ones - how plant lipid droplets connect with other subcellular structures. New Phytol 2022;236: 833-8.
58. Thazar-Poulot N, Miquel M, Fobis-Loisy I, Gaude T. Peroxisome extensions deliver the Arabidopsis SDP1 lipase to oil bodies. Proc Natl Acad Sci USA 2015;112:4158-63.
59. Goto T, Lee JY, Teraminami A, Kim YI, Hirai S, Uemura T, et al. Activation of peroxisome proliferator-activated receptor-alpha stimulates both differentiation and fatty acid oxidation in adipocytes. J Lipid Res 2011;52:873-84.

Received: 6 April 2026. Accepted: 1 July 2026.

This work is licensed under a Creative Commons Attribution-NonCommercial 4.0 International License (CC BY-NC 4.0).
©Copyright: the Author(s), 2026
Licensee PAGEPress, Italy
European Journal of Histochemistry 2026; 70:4574
doi:10.4081/ejh.2026.4574

Publisher's note: all claims expressed in this article are solely those of the authors and do not necessarily represent those of their affiliated organizations, or those of the publisher, the editors and the reviewers. Any product that may be evaluated in this article or claim that may be made by its manufacturer is not guaranteed or endorsed by the publisher.